STM JOURNALS

Journal of
Polymer & Composites

http://engineeringjournals.stmjournals.in/index.php/JoPC/index

ISSN: 2321-2810 (Online)
ISSN: 2321-8525 (Print)
Volume 12, Special Issue 2, 2024
DOI (Journal): 10.37591/JoPC

Research JoPC

# Parametric Optimization and Validation of Novel 3D Scanning Approach for Sustainable Manufacturing of Patient-Specific Orthodontic Retainers

Sumit Gahletia[1,*], Ramesh Kumar Garg[2]

***Abstract***

*The purpose of the proposed study is to identify the ideal procedure parameters for 3D scanning a denture in order to produce customised orthodontic retainers that can be produced sustainably. However, pilot investigations rarely explore parameters like scanning angle, light intensity, or scanning distance. In order to lower acquisition error, the suggested study examines a method for forecasting the ideal values of the previously indicated scanning parameters. Based on the fundamental face-centered composite design, twenty testing iterations with various input parameter settings were suggested. From a physical denture model, each of these 20 scans was utilised to create a 3-D CAD model. The standard deviation of each model was computed to assess the accuracy of the data gathered. RSM's utilisation of the standard deviation enables parametric optimisation for increased scan model accuracy. The best accuracy has been demonstrated experimentally by the RSM method at 8.33 inches of scanning distance, 65.61 degrees of angle, and 17.27 watts per square metre of light.*

**Keywords**: 3D scanning, process optimization, central composite design, response surface methodology, data acquisition

## INTRODUCTION

More precise measurement and imaging of the teeth and related soft tissues are now needed than ever before for the diagnosis and treatment of temporomandibular disorders. Even though 3D digitization technologies have advanced significantly, the traditional method of taking dental cast imprints in order to create occlusal appliances has not yet been fully superseded by these technologies [1,2]. As opposed to traditional impressions, which showcase the negative representations of constructed teeth, the outcome of 3D digitization is data that maps the 3D coordinates of the object [3,4]. This is in contrast to the traditional impression techniques. One of these measuring techniques has the capability of utilizing many operating principles in order to improve the treatment process [5, 6]. In order to obtain accurate 3D scans for the purpose of designing custom occlusal appliances, dental professionals face a number of challenges. The lack of optical properties on the tooth surface, the wet oral environment, the need for matting powder, the presence of the camera and patient movements during the 3D digitization process, and the size restriction on the digitised region are some of these problems [7–11]. One of the most important issues to deal with throughout the laser scanning process is how to choose the right process variables so that the entire scan may be completed in the fewest steps feasible. For the parameters of the input process, such as the scanning angle, light intensity, and scanning distance, a range of choices is always

***Author For Correspondence**
Sumit Gahletia

[1]Research Scholar, Mechanical Engineering Department, Deenbandhu Chhotu Ram University of Science and Technology, Murthal, Sonipat, Haryana, India
[2]Professor, Mechanical Engineering Department, Deenbandhu Chhotu Ram University Of Science And Technology, Murthal, Sonipat, Haryana, India

Received Date: March 21, 2024
Accepted Date: April 04, 2024
Published Date: May 16, 2024

**Citation:** Sumit Gahletia, Ramesh Kumar Garg. Parametric Optimization and Validation of Novel 3D Scanning Approach for Sustainable Manufacturing of Patient-Specific Orthodontic Retainers. Journal of Polymer & Composites. 2024; 12(Special Issue 2): S265–S278p.

 

available. Even though they are not always obvious, these decisions have a significant impact on the scan outcomes. Therefore, it is crucial to set up ideal process conditions and use scanner professionals to tweak vital process parameter values for the greatest possible benefit. [12–16]. In addition, it is essential to have an understanding of the process variables and user-based decision factors that optical scanning equipment can implement in order to achieve the highest possible level of accuracy. In Figure 1, a complete breakdown of the numerous components that are involved in the scanning process is depicted.

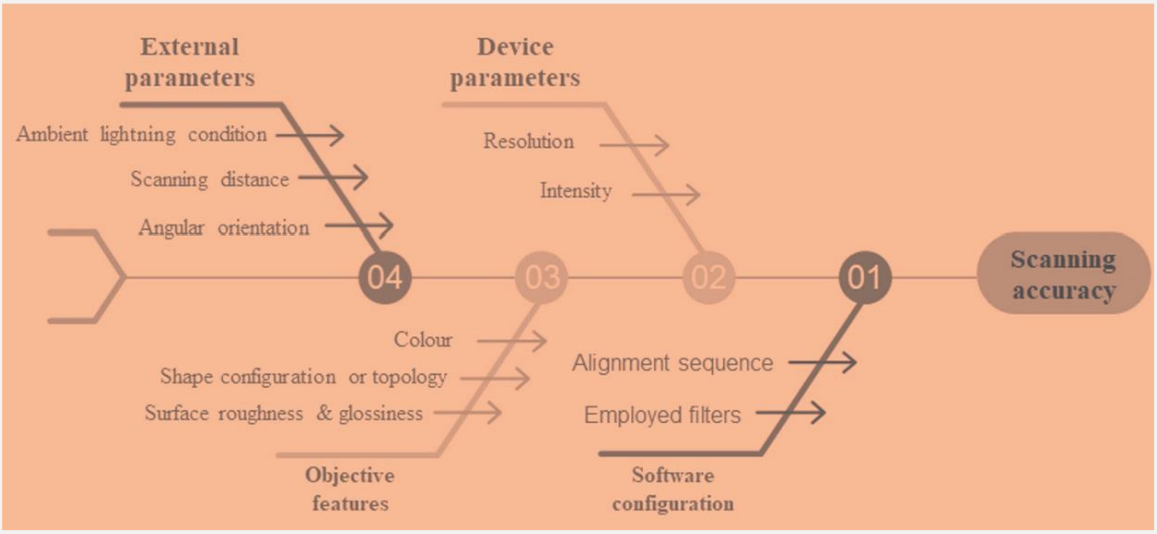


**Figure 1.** Fish bone analysis of 3D scanning parameters

## MEASUREMENT SYSTEM

Triangulation-based laser stripe systems are widely used in metrology due to their high accuracy, low cost, and ease of installation. A CCD sensor detects many points of the stripe that are produced on the surface when a specific angular width incident laser line is projected onto the component to be scanned [17–19]. The 3D coordinates of the surface locations are then calculated using the triangulation technique. As demonstrated in Figure 2, the range may differ from scanner to scanner based in part on the lens, focus distance, and selected optics. Following are a few terms' definitions.

Figure 2 illustrates several geometrical aspects of these measurement methods, some of which are purely reliant on the optical, types of lenses, and distance of focus points, so the range can vary if compared with different types of scanners.

i. *FOV [mm] (Field of view):* 3D space where points from the scanned surface can be collected by the CCD sensor.
ii. *(DOF) [mm]Depth of focus*: the distance between the laser source and the CCD sensor that the CCD sensor may employ to take pictures of areas on the surface being scanned that are normally connected to the lens.
iii. *Scan width (mm):* laser beam width as measured at the midpoint of the depth of field. The visible portion is the only one that gets measured.
iv. *D [mm]Stand-off distance*: This measurement measures the distance between the laser source and a benchmark surface that is located in the centre of field and is dependent on the opticals and lenses focus.
v. *The angle, measured in degrees:* between the laser beam that is incident on the scanning plane and the surface that is perpendicular to the scanned point.
vi. *Angle that is projected (in degrees):* between the scanning plane and the surface's normal at the scanned location.

 

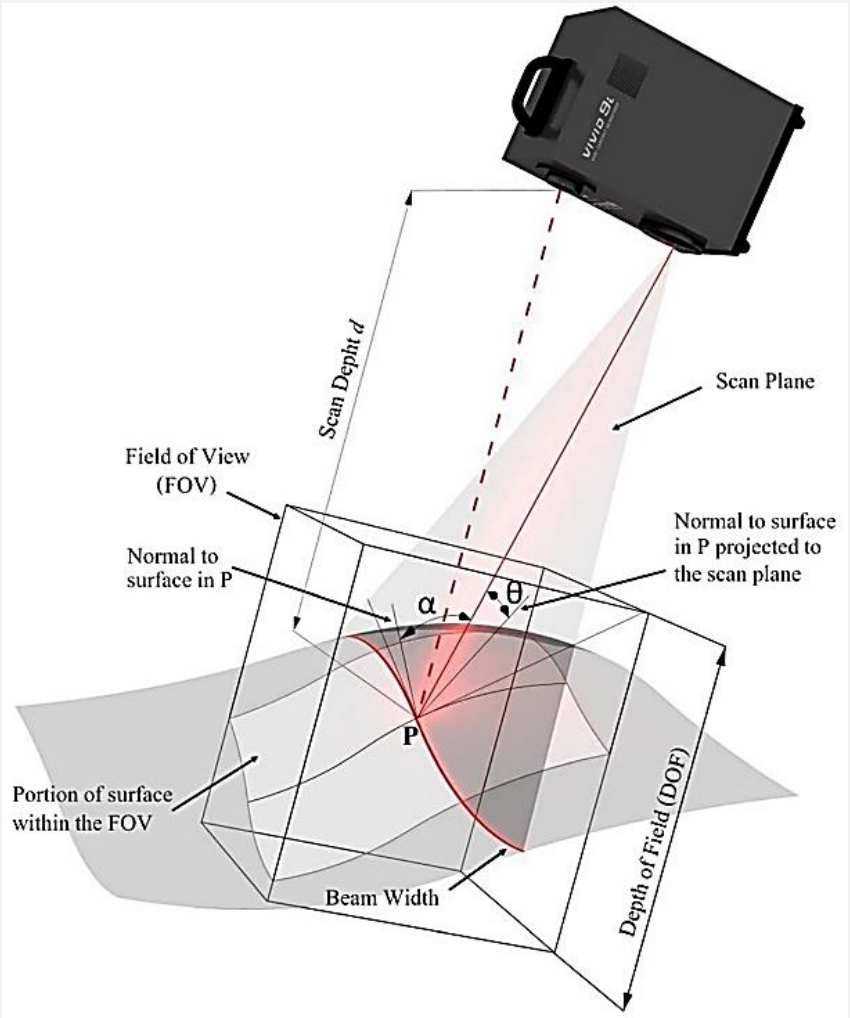


**Figure 2.** Important optical scanner parameters and their layout in a simplified diagram

Martinez et al.,2010 explained the evaluation of CMM touch probe of digitising against CMM laser digitising with the intent of investigating the impact of component shape on the results of laser scanning. It is advised to use large-diameter reference spheres positioned as far away from the data sets as possible. The results of the study show that a variety of scanning characteristics, including ambient lighting, laser intensity, focus distance, and the number of collected points, have a direct impact on how accurate the scanning approach is. However, compared to employing numerous scanning head configurations, accuracy is enhanced when these parameters are held constant and a single scanning head placement is used. The findings are unique to CMM laser scanners, which offer more control than portable laser scanners, which are used more frequently. It can be difficult to determine the distance and scanning direction of mobile scanners at a fixed value since they can vary significantly during the scanning process. In addition, portable 3D scanners are often more vulnerable to variations in light intensity [20]. The presence of natural daylight greatly influences the optical measurements. The versatility of existing 3D scanners, manufactured by different companies, to operate well under varying levels of light intensity was highlighted. However, many customers still maintain that they are prone to sensitivity issues during practical usage. An analysis was conducted using a laser scanner to investigate different types of materials that had undergone the same surface treatment [21]. Mercury vapour lamps yielded superior outcomes compared to halogen illumination due to their reduced variability and increased availability of data. The main results of this study indicate that maintaining an uninterrupted and minimum distance between the scanner and typodont model is necessary, to reduce interference and enhance the amount of data collected.[22].

 

According to research conducted by several authors [23–25], the most optimal situation occurred when the laser scanner was correctly positioned in respect to the surface. This study specifically focused on evaluating the efficacy of laser scanners in different orientations relative to the surface. For free-form surfaces, it might be impossible or extremely difficult to do this. A meticulously choreographed trajectory of the scanner encompassing the whole of the item will be designed.

The proposed study aims to use a 3D laser scanner to rebuild a dental model and assess its correctness by analysing the impact of different input elements and their interactions. Three main input factors, namely light intensity, scanning distance and scanning angle, were utilised to scan a denture model utilising a hand-held 3D laser scanner. A total of twenty experiments have been generated utilising a composite-design called FCC, which involves numerous combinations of input elements. Therefore, twenty CAD models have been produced by considering twenty alternative combinations of input factors. The standard deviation, which is used as an end answer, is used to check if the scan model is right. There is a link between input and output that was set up with the help of a neural network. Because of this, a genetic formula has been used to make it even better.

**Materials and Methods**

The following steps can be used to characterise the methodology (Figure 3) that was utilised to select an experimental design, identify process factors, identify an objective, carry out the design, and analyse the results in order to determine the optimal scanning parameters through the use of Design of Experiments (DoE). The problem is defined and stated in accordance with the user's goal right away.

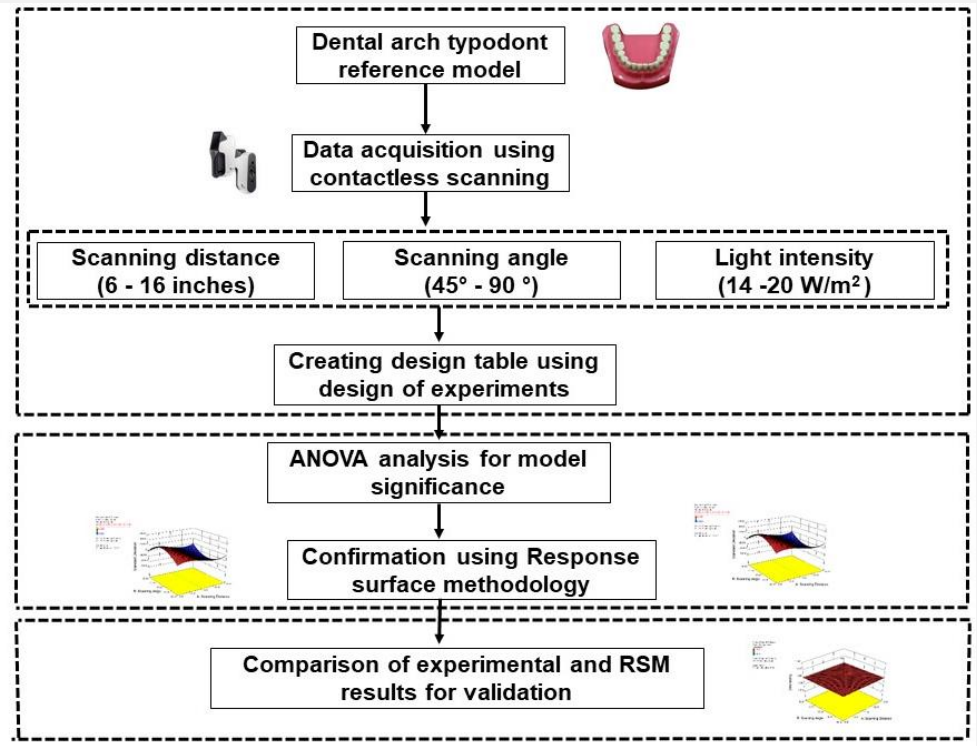


**Figure 3.** Methodology utilized to achieve optimal scanning parameters.

Setting priorities for goals will help researchers and academicians to work towards defining the range of process variables, such as input and output reactions. The selection of an effective experimental strategy is influenced by the experiment's objective and the quantity of components that require investigation. Because it can link and build the form of the response surface that is utilised for testing, the response surface method with a central composite design approach is employed in the suggested study. Data interpretation and analysis are used to test data and the accompanying research to ensure

 

that everything aligns with the objectives. Because hyperspace analysis covers a larger area, using a range of scanning parameters is necessary to guarantee thorough scanning of the entire item. Three important but little-studied variables—light intensity, scanning distance, and scanning angle—are the focus of the proposed study. A detailed examination of the current literature served as the foundation for this study.

Using a face-centred composite design approach, the impact of operational variables was examined. nc centre runs, 2n axial runs, and 2n factorial runs make up the current strategy. Centre points control the replication of data, and experimental error equation 1 was utilised to forecast the number of necessary experimental runs.

$N = 2^n+2n+nc$ (1)

So, N is the total number of runs, nc is the number of the centre point, and n is the number of process factors. According to the current method, the optimisation process needs twenty experimental runs, which are made up of eight factorial experiments, six axial experiments, and six middle trials.

***Experimental planning***

The dental model, as shown in Figure 4, is often used for simulating dental treatments. It consists of sixteen teeth and is employed to investigate the correlation between different scanning parameters and the resulting output response. The proposed study use the Calbiry small 3D scanner, which is particularly designed for collecting human anatomical parts and prototypes, to acquire data and conduct optical scanning experiments. The Calbiri small scanner has a point resolution of roughly 0.15mm and a field of view ranging from 86*115mm to 144*192mm.

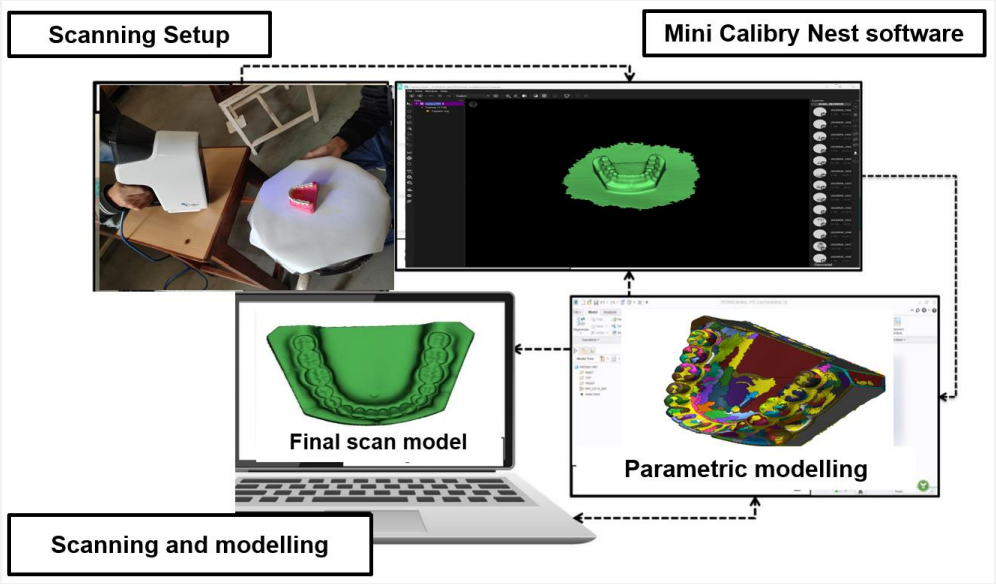


**Figure 4.** Layout of experimental setup for 3D scanning

The typodont model is positioned on a rotating table to achieve the desired rotational movement while maintaining a steady position for the scanner. Using a light intensity metre to measure the amount of light in the area and a gyroscope-based sensor on the smartphone to figure out the scanner's geometrical angles. The suggested investigation encompasses a measurement field that spans from 100 mm to 400 mm. The measuring volume of a field of vision with a width of 100 mm is 120 mm in length, 100 mm in width, and 60 mm in height. There is a variation in the field of vision between the 400 mm and 200 mm measurement field. The part is moved around on a moving table so that different scans can be done with different process settings. The surface was copied after each scan with the Calbri nest tool.

 

The typodont model is positioned on a revolving table that may swivel, allowing for gradual rotation. The scanner's tilt can be adjusted between 45 degrees and 90 degrees. The ambient light intensity throughout the experiment ranged from 14 to 20 W/m$^2$. The scanning range for individual scanning using the scanner is from 6 to 16 inches. The DoE approach is used to get the desired parametric combination by eliminating needless testing and focusing on the important parameters that have the greatest influence on the result.

## CENTRAL COMPOSITE DESIGN APPROACH

A Central composite design approach consists of a fractional factorial design or an imbedded factorial function having centre points augmented with a bunch of star points for to facilitate the estimation of curvature as represented in Figure 5. When |alpha| > 1, the distance from origin to factorial point is +1. Otherwise, the distance of origin to star point is -1. The total number of center point runs that the design must include also depends on specific features that are necessary for the design.

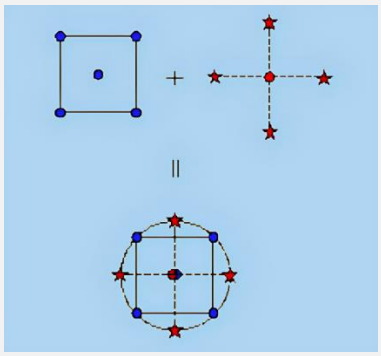

**Figure 5.** Designing of central composite model

Scanned distance (A), scanning angle (B), and light-intensity (C) are three process variables were considered to attain the ideal conditions. The current method consists of 2n factorial trials, nc centre simulations, and 2n axial simulations. Centre points regulate reproducibility of data and experimental error [26]. Using Eq. (1), we can determine how many times we'll need to do our experiments.

$$N = 2n+2n+nc \quad (1)$$

N stands for total no of runs, C stands for the centre point, and n stands for the quantity of process components. The present approach to optimisation calls for 6 axial experiments, 8 factorial trials, and 6 centred experiments. Figure 6 depicts the generalized flowchart of DoE analysis.

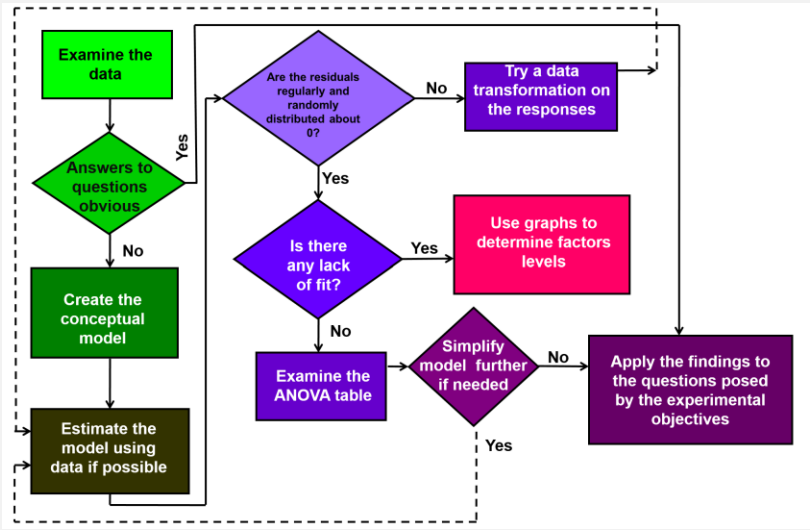


**Figure 6.** Generalised flow chart for DoE data analysis

 

Twenty scan tests were done using a parametric mixture made with DoE as represented in Figure 7. To determine accuracy of scanning at significant parameters, the standard deviation is used as the output variable. Because of its statistical significance, ability to effectively analyse sensitivity, and enhanced quality control, standard deviation is chosen as the output response for evaluating the impacts of scanning settings. A standard deviation measures how far the point cloud data is from the mean and is therefore a defining feature of the data. Scan the data surface according to the catalogue's directions, and then compare it to the stl file you created during your pilot experiments to get an idea of the average difference. It refers to how well measurements hold up when compared to the mean and how consistent the findings are. The quantity of points should be sufficiently limited to provide efficient management and fast processing, while also comprehensively including all pertinent characteristics. The main purpose of Geomagic Control X programme is to perform inspections and record measures of standard deviation. The efficacy of the stated parameters in enhancing the scan quality may be shown if the scan collected with these parameters exhibits higher standards and better precision compared to the scan obtained without any parameters. On the other hand, if the results from the two scans are quite similar, it might mean that the parameters you've supplied aren't needed or that you need to tweak some other settings to get a better scan. By comparing scans taken with and without certain factors, one may assess the efficacy of scan parameters.


**Figure 7.** Twenty CAD models retrieved as per the parametric combination obtained using DoE methodology

## RESULTS AND DISCUSSION

The (20×3) anticipated CCD input variable matrix has been patched with the (20×1) empirically acquired output variable matrix in order to continue with the (20×4) input-output matrix for RSM training analysis. Using a polynomial model of quadratic order to determine the percentage of design space, RSM expedites the evaluation towards the optimization target. A legitimate lack of fit test has been performed throughout the RSM model evaluation, as evidenced by the lack of fit value.

### Fit Output Response Model Summary and Anova

The output response for each experiment was measured and recorded in accordance with the RSM-based FCCCD. In the summary, cubic-model was an alias for the polynomial vs. two-factor interaction model, which was recommended for a precise fit of the design. ANOVA (quadratic model) findings for standard deviation showed that the model was statistically significant and precise enough ($R^2$(SD)=0.9890) to allow for continued navigation over unknown inputs using regression equation 1 listed below. A description of the model's fit is provided in Table 1.

 

**Table 1.** Output response characteristics summary obtained using ANOVA

| **Std. Dev.** | **0.020972903** | **R-Squared** | **0.98903655** |
|---|---|---|---|
| C.V. % | 5.587112566 | Pred R-Squared | N/A |
| Mean | 0.37538 | Adj R-Squared | 0.958338891 |
| PRESS | N/A | Adeq Precision | 21.41708785 |

It is always advised to select the highest order polynomial model. For all the standard deviation as output response, the lack of fit for the cubic regression analysis is "significant" in the current scenario. Since then, it is recommended to use a quadratic model for the output response. A procedure similar to removal by backwards classification was used to get rid of terms which does not have a considerable impact. $R^2$(Adjusted and Predicted), a test to determine the impact of the regression-based model, and their coefficients are all included in the ANOVA given for the output response measurements in Table 2.

***Equation For Regression in Actual Terms***

The following diagram illustrates the regression equation for calculating output response from input scanning parameters:

$$\begin{aligned} Standard\ Deviation \\ &= 0.302233333 - 52012.90592 * A0.032019402 * B - 0.00166489 * C \\ &- 0.011137735 * A * B - 0.010737708 * A * C - 0.016187673 * B \\ &* C0.02558548 * A\text{^}20.104480919 * B\text{^}20.049521045 * C\text{^}2 \\ &- 0.029712711 * A * B * C - 0.033132111 * A\text{^}2 * B - 0.017197849 \\ &* A\text{^}2 * C33623.61748 * A * B\text{^}2 \end{aligned}$$

**Table 2.** Characteristics of ANOVA's output response

| **Source** | **Sum of Squares** | **D f** | **Mean Square** | **F Value** | **p-value Prob > F** | |
|---|---|---|---|---|---|---|
| Model | 0.198404819 | 14 | 0.014171773 | 32.21863058 | 0.0006 | significant |
| A-Scanning Distance | 0.048875791 | 1 | 0.048875791 | 111.116025 | 0.0001 | |
| B-Scanning Angle | 0.005799645 | 1 | 0.005799645 | 13.18512672 | 0.0150 | |
| C-Light Intensity | 1.568E-05 | 1 | 1.568E-05 | 0.035647492 | 0.8577 | |
| AB | 0.000992391 | 1 | 0.000992391 | 2.256138234 | 0.1934 | |
| AC | 0.000922371 | 1 | 0.000922371 | 2.096952518 | 0.2073 | |
| BC | 0.002096307 | 1 | 0.002096307 | 4.765821912 | 0.0808 | |
| A^2 | 0.007855402 | 1 | 0.007855402 | 17.85875971 | 0.0083 | |
| B^2 | 0.13099515 | 1 | 0.13099515 | 297.8092036 | < 0.0001 | |
| C^2 | 0.029428007 | 1 | 0.029428007 | 66.90271509 | 0.0004 | |
| ABC | 0.007062661 | 1 | 0.007062661 | 16.05651442 | 0.0103 | |
| A^2B | 0.003637546 | 1 | 0.003637546 | 8.269731309 | 0.0348 | |
| A^2C | 0.000980067 | 1 | 0.000980067 | 2.228120963 | 0.1957 | |
| AB^2 | 0.04887595 | 1 | 0.04887595 | 111.1163871 | 0.0001 | |
| AC^2 | 0 | 0 | | | | |
| B^2C | 0 | 0 | | | | |
| BC^2 | 0 | 0 | | | | |
| A^3 | 0.048875839 | 1 | 0.048875839 | 111.1161345 | 0.0001 | |
| B^3 | 0 | 0 | | | | |
| C^3 | 0 | 0 | | | | |
| Pure Error | 0.002199313 | 5 | 0.000439863 | | | |
| Cor Total | 0.200604132 | 19 | | | | |

 

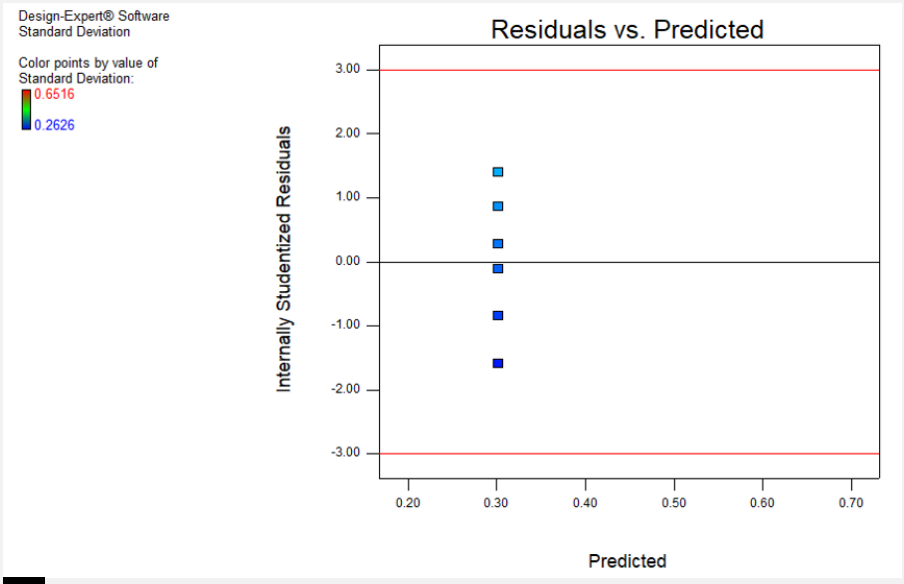


(a)

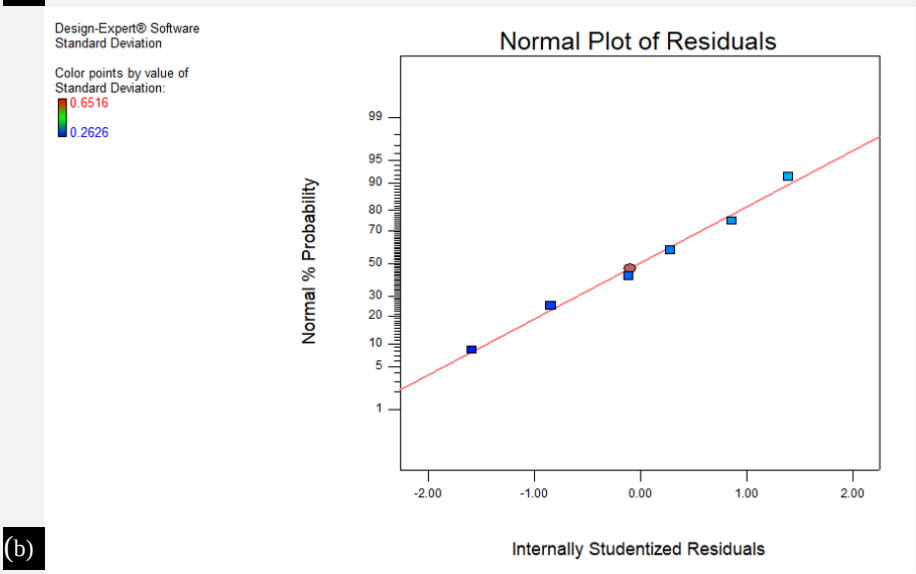


(b)

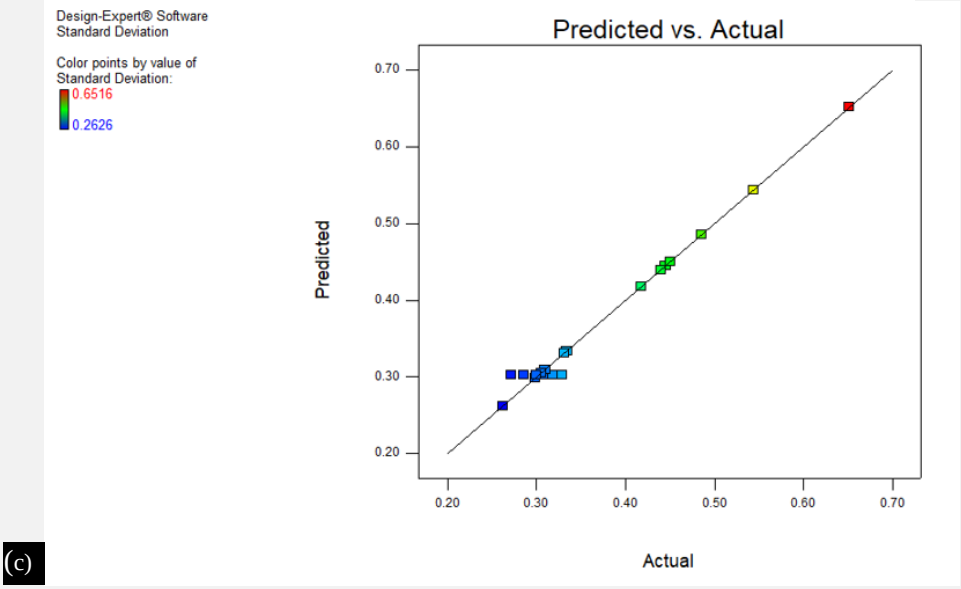


(c)

 

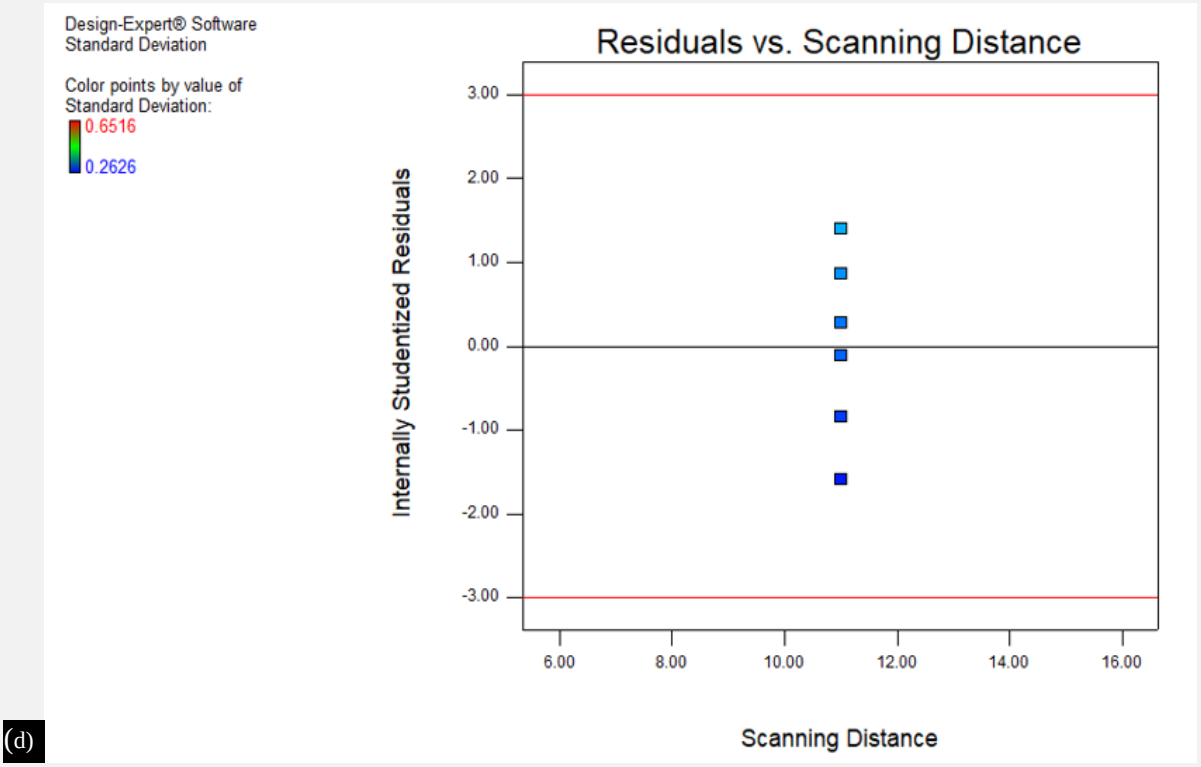


**Figure 8.** (a) Residual vs predicted plot (b) normal plot of residuals, (c) predicted vs actual plot ,(d) plot of residual vs scanning distance

**RESIDUAL VS PREDICTED PLOT**

The residual vs predicted plot, while the y-axis shows the residuals, which are the discrepancies between the actual and expected values, and the x-axis displays the anticipated values from the model, is used to assess the accuracy of the statistical model employed in the suggested research. The residuals should be randomly distributed around the horizontal line at zero for best results, demonstrating that the model's predictions are reasonable and accurate as shown in figure 8(a).

**Normal Residual Plot**

The residuals' normality assumption is evaluated using the normal plot. The theoretical quantiles of a normal distribution are plotted against the ordered residuals. If the data points fall approximately along a straight line as depicted in figure 8(b), it indicates that the normal distribution, which is a crucial assumption in many statistical analyses. Departures from normality may indicate that the statistical model needs further investigation or possible transformations.

***Predicted Versus Actual Plot***

The predicted versus actual plot visual representation of how accurate the model's predictions match the actual observed values. The y-axis showing the predicted values across the model, and the x-axis displaying the corresponding actual values. The points in figure 8 (c) approximately lie along the diagonal line, indicating perfect agreement between predictions and actual outcomes.

**Plot Of Residual Vs Scanning Distance**

This plot investigates the relationship between the residuals and scanning distance, focusing on any potential systematic patterns or trends. The x-axis represents the scanning distance values, while the y-axis displays the corresponding residuals. This analysis helps identify whether certain scanning distances lead to larger or smaller discrepancies between predicted and actual values and it is evident from figure 8 (d), that scanning distance significantly influences the accuracy of the model's predictions.

 

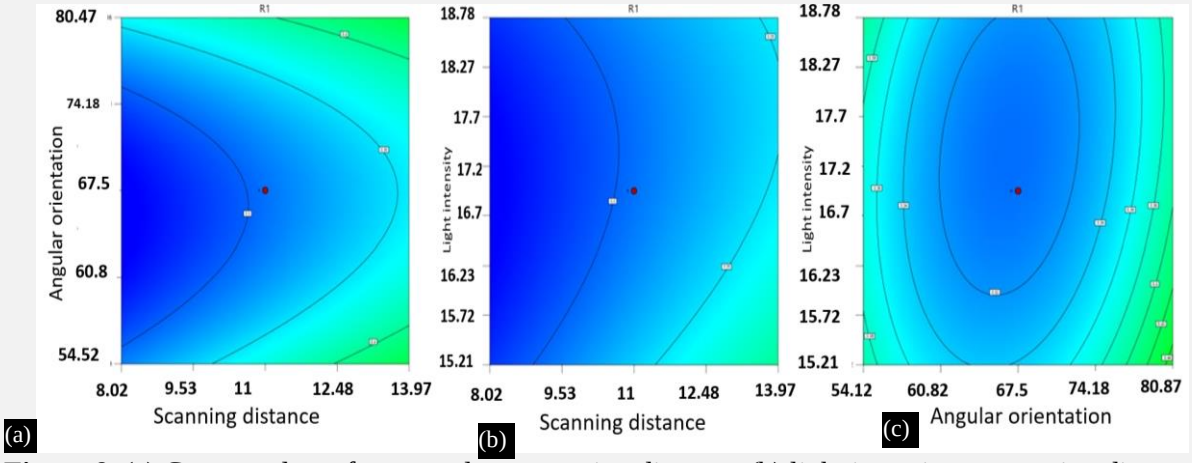


**Figure 9.** (a) Contour plots of scan angle vs scanning distance, (b) light intensity vs scanning distance, (c) scan angle vs light intensity

Contour plots are graphical representations that vividly illustrate the relationship among different process parameters. These contour plots provide valuable insights into the interaction and effects of these parameters on the scanning process for dental models using a hand-held 3D scanner. The contour plot depicting scan angle versus scanning distance in figure 9 (a) demonstrates the relationship between these two parameters and their impact on scanning accuracy and efficiency. The x-axis signifies the scanning distance, while the y-axis stands for the scan angle. The contour lines on the plot indicate regions of equal scanning performance. For example, areas with denser contour lines suggest a more robust and consistent scanning outcome, while sparser contours may indicate regions of potential scanning challenges or inaccuracies. These helps in identification of the optimal combination of scan angle and scanning distance that yields the highest quality and precision in the scanned dental models.

In figure 9 (b) the contour plot, explore the relationship between light intensity and scanning distance, two crucial factors influencing the overall scanning process. The x-axis portrays the scanning distance, while the y-axis represents the light intensity. Similar to the previous plot, the contour lines delineate regions of equal scanning performance, which helps to determine the ideal balance between light intensity and scanning distance for optimal scanning results. Regions of higher contour density suggest settings that yield superior scanning outcomes, while areas with sparse contours indicate settings that may result in scanning difficulties or inconsistencies.

Contour plot in Figure 9(c) explores the relationship between scan angle and light intensity and their joint influence on the scanning process. The x-axis signifies the scan angle, while the y-axis stands for light intensity. The contour lines reveal the combinations of scan angle and light intensity that result in the most favourable scanning outcomes. The regions with denser contour lines, indicates the configurations that achieve high scanning accuracy and efficiency, while regions with sparse contours may point to settings that are less conducive to achieving optimal results. This comprehensive analysis of the contour plots aids in drawing meaningful conclusions and guiding future research directions in the field of digital dentistry and hand-held 3D scanning technology.

## 3D SCANNING PARAMETERS EFFECT ON OUTPUT RESPONSE

The 3D model of the variation of scanning angle and scanning distance is represented in Figure 10(a) which depicts how variations in these two parameters affect the measured outcome. It illustrates the complex relationship between scanning angle and distance and their combined impact on the accuracy of scan models. The graph reveals that standard deviation decreases with decrease in scanning angle and scanning distance to a certain point and then begins to increase. The interaction of scanning distance with light intensity is represented in Figure 10(b) which clearly illustrates that standard deviation increase with light intensity and scanning distance. The interaction of scanning angle and light intensity

 

is demonstrated in figure 10(c) which emphasize the significant effects of light intensity on the study outcomes and how it interacts with scanning angle to shape the outcome. The RSM 3D evaluation plot as represented in figure 10(d) provides a visual representation of how the response variable ie standard deviation change concerning two input variables (scanning distance and scanning angle). Ramp function plot for optimized parametrs for combined parametric optimization is demonstrated in figure 11(a).

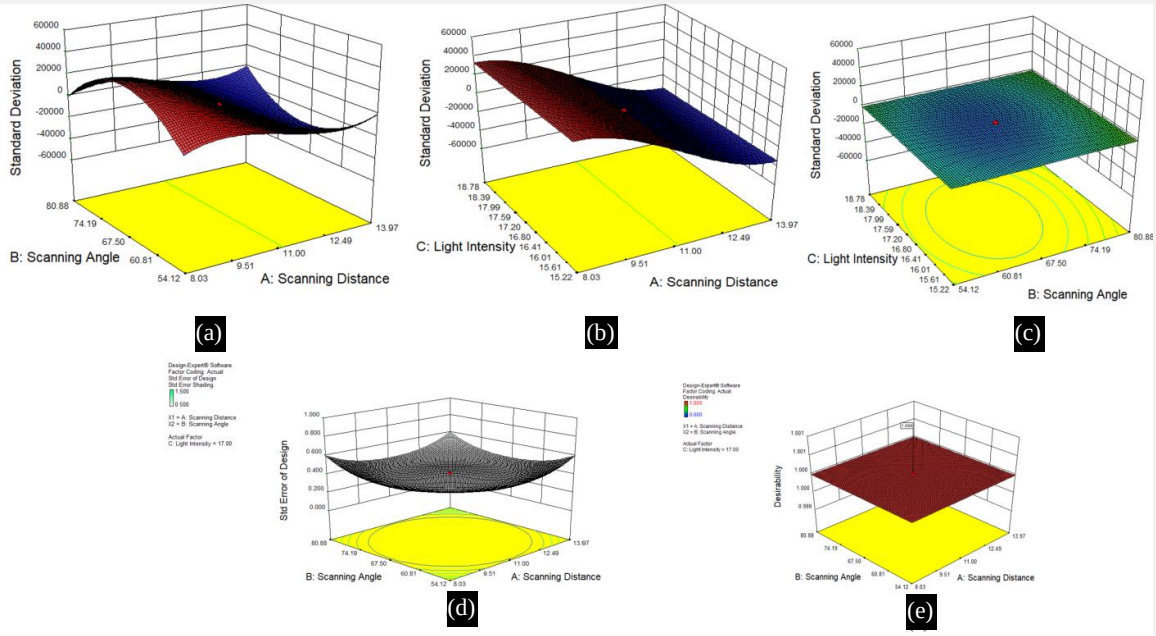


**Figure 10.** (a) Variation of scanning angle and scanning distance, (b)Variation of scanning distance and light intensity, (c)Variation of scanning angle and light intensity, (d)RSM 3D evaluation plot ,(e) RSM optimization plot

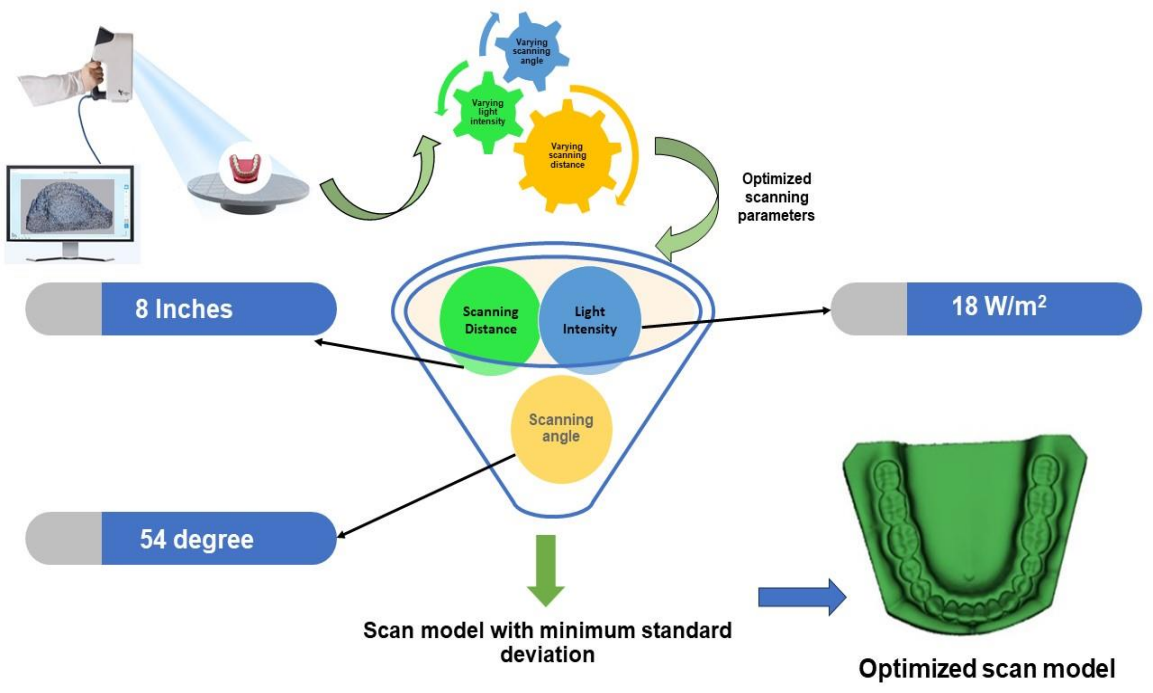


**Figure 11.** (a) RSM optimization results, (b) Bar graph for desirability for combined parametric optimization

 

**Comparison And Verification of Optimisation Methods**

The model was subsequently validated utilising validation trials with a 3D scanner. Using the best RSM results available, confirmation tests will been conducted at 3 variables (scanning angle, light intensity, and scanning distance. The output answers are compared and summarised in Table 3. An average value is used to conduct each set of tests in order to maintain accuracy. Confirmation studies' findings demonstrated how closely the experimental and predicted values matched

**Table 3.** Comparison and verification of RSM optimisation method

| Technique | Input Parameters | | | Experimental Standard Deviation | Predicted Standard Deviation | Percentage error |
|---|---|---|---|---|---|---|
| RSM | Scanning Distance | Scanning Angle | Light Intensity | | | |
| | 8.33 inches | 54.61 degree | 18 W/m$^2$ | 0.2621 | 0.2617 | 15.28 % |

## CONCLUSION

The proposed research aimed to optimize the process parameters for scanning dental models using a hand-held 3D scanner. Through a systematic evaluation of significant parameters, it was determined that each parameter plays a significant role in the quality and accuracy of the scanned dental models. The study indicate that optimizing these parameters helps to minimize the occurrence of motion artifacts, ensure a smooth scanning process and enhance the level of detail captured in the dental models, resulting in more accurate scan models. The minimum standard deviation of the 3D scanner's input parameters has been calculated. The trials were conducted using the Face Central Composite Design (FCCD) technique. The best accuracy was found in Experiment Model M1, where the standard deviation was 0.2626 while using a scanning distance of 8.02 inches, a scanning angle of 54.12 degrees, and a light intensity of 18.78 watts per square meter. Standard deviation-based parametric optimization is used by RSM to improve scan model accuracy. Standard deviation is reduced to 0.02617 using the RSM method at a scanning distance of 8.3 inches, an angle of 65.61 degrees, and a light intensity of 17.72 watts per square meter. This optimization can lead to improved diagnosis, treatment planning, and fabrication of dental prostheses. By accurately capturing the dental anatomy, clinicians and technicians can better assess the oral condition, design customized prostheses, and ensure a precise fit. However, the optimization of process parameters is not a one-size-fits-all approach, as different dental models may require specific parameter settings. Therefore, further studies should focus on developing adaptive algorithms or intelligent software that can automatically adjust the process parameters based on the scanned object's characteristics.

## REFERENCES

1. Singh R, Kumar A, Boparai KS. Additive Manufacturing Assisted Preoperative Surgical Planning for Canine Femur Bone Fracture. National Academy Science Letters. 2022 Dec;45(6):521-4.
2. Kaushik A, Gahletia S, Garg RK, Sharma P, Chhabra D, Yadav M. Advanced 3D body scanning techniques and its clinical applications. In2022 International Conference on Computational Modelling, Simulation and Optimization (ICCMSO) 2022 Dec 23 (pp. 352-358). IEEE.
3. Kovacs L, Zimmermann A, Brockmann G, Gühring M, Baurecht H, Papadopulos NA, Schwenzer-Zimmerer K, Sader R, Biemer E, Zeilhofer HF. Three-dimensional recording of the human face with a 3D laser scanner. Journal of plastic, reconstructive & aesthetic surgery. 2006 Nov 1;59(11):1193-202.
4. Aung SC, Ngim RC, Lee ST. Evaluation of the laser scanner as a surface measuring tool and its accuracy compared with direct facial anthropometric measurements. British journal of plastic surgery. 1995 Jan 1;48(8):551-8.
5. Istook CL, Hwang SJ. 3D body scanning systems with application to the apparel industry. Journal of Fashion Marketing and Management: An International Journal. 2001 Jun 1;5(2):120-32.
6. Haleem A, Javaid M. 3D scanning applications in medical field: a literature-based review. Clinical Epidemiology and Global Health. 2019 Jun 1;7(2):199-210.
7. Feng HY, Liu Y, Xi F. Analysis of digitizing errors of a laser scanning system. Precision Engineering. 2001 Jul 1;25(3):185-91.

 

8. Bush K, Antonyshyn O. Three-dimensional facial anthropometry using a laser surface scanner: validation of the technique. Plastic and reconstructive surgery. 1996 Aug 1;98(2):226-35.
9. McCarthy JG, Karron DB. Three-dimensional input of body surface data using a laser light scanner. Annals of plastic surgery. 1988 Jul 1;21(1):38-45.
10. Peiravi A, Taabbodi B. A reliable 3D laser triangulation-based scanner with a new simple but accurate procedure for finding scanner parameters. Journal of American Science. 2010 May 12;6(5):80-5.
11. Napolitano P, Alimenti F, Carbone P. A novel sample-and-hold-based time-to-digital converter architecture. IEEE Transactions on Instrumentation and Measurement. 2010 Mar 29;59(5):1019-26.
12. Cuesta E, Rico JC, Fernández P, Blanco D, Valiño G. Influence of roughness on surface scanning by means of a laser stripe system. The International Journal of Advanced Manufacturing Technology. 2009 Aug; 43:1157-66.
13. Vukašinović N, Možina J, Duhovnik J. Correlation between incident angle, measurement distance, object colour and the number of acquired points at CNC laser scanning. Strojniški vestnik-Journal of Mechanical Engineering. 2012 Jan 15;58(1):23-8.
14. Ouji K, Ardabilian M, Chen L, Ghorbel F. 3D deformable super-resolution for multi-camera 3D face scanning. Journal of mathematical imaging and vision. 2013 Sep; 47:124-37.
15. Stančić I, Musić J, Zanchi V. Improved structured light 3D scanner with application to anthropometric parameter estimation. Measurement. 2013 Jan 1;46(1):716-26.
16. Martínez S, Cuesta E, Barreiro J, Álvarez B. Analysis of laser scanning and strategies for dimensional and geometrical control. The International Journal of Advanced Manufacturing Technology. 2010 Jan; 46:621-9.
17. Isa MA, Lazoglu I. Design and analysis of a 3D laser scanner. Measurement. 2017 Dec 1; 111:122-33.
18. Pathak VK, Singh AK. Optimization of morphological process parameters in contactless laser scanning system using modified particle swarm algorithm. Measurement. 2017 Oct 1; 109:27-35.
19. Schwarz-Müller F, Marshall R, Summerskill S, Poredda C. Measuring the efficacy of positioning aids for capturing 3D data in different clothing configurations and postures with a high-resolution whole-body scanner. Measurement. 2021 Feb 1; 169:108519.
20. Martínez S, Cuesta E, Barreiro J, Alvarez B. Methodology for comparison of laser digitizing versus contact systems in dimensional control. Optics and Lasers in Engineering. 2010 Dec 1;48(12):1238-46.
21. Blanco Fernández D, Fernández Álvarez P, Cuesta González E, Mateos Díaz S, Beltrán Delgado N. Influence of surface material on the quality of laser triangulation digitized point clouds for reverse engineering tasks. In Emerging Technologies & Factory Automation, 2009 ETFA 2009 IEEE Conference on 2009.
22. Lartigue C, Contri A, Bourdet P. Digitised point quality in relation with point exploitation. Measurement. 2002 Oct 1;32(3):193-203.
23. Contri A, Bourdet P, Lartigue C. Quality of 3D digitised points obtained with non-contact optical sensors. CIRP Annals. 2002 Jan 1;51(1):443-6.
24. Mahmud M, Joannic D, Roy M, Isheil A, Fontaine JF. 3D part inspection path planning of a laser scanner with control on the uncertainty. Computer-Aided Design. 2011 Apr 1;43(4):345-55.
25. Feng HY, Liu Y, Xi F. Analysis of digitizing errors of a laser scanning system. Precision Engineering. 2001 Jul 1;25(3):185-91.

 